



## ORIGINAL ARTICLE

# The Superficial White Matter in Autism and Its Role in Connectivity Anomalies and Symptom Severity

Seok-Jun Hong <sup>1,2</sup>, Brian Hyung<sup>1</sup>, Casey Paquola<sup>1</sup> and Boris C. Bernhardt<sup>1</sup>

<sup>1</sup>Multimodal Imaging and Connectome Analysis Laboratory, McConnell Brain Imaging Centre, Montreal Neurological Institute and Hospital, McGill University, Montreal, QC H3A 2B4, Canada and <sup>2</sup>Center for the Developing Brain, Child Mind Institute, 101 E 56th St, New York, NY 10022, USA

Address correspondence to Boris Bernhardt, Multimodal Imaging and Connectome Analysis Laboratory, McConnell Brain Imaging Centre, Montreal Neurological Institute and Hospital, McGill University, Montreal, QC, Canada. Email: boris.bernhardt@mcgill.ca; Seok-Jun Hong, Multimodal Imaging and Connectome Analysis Laboratory, McConnell Brain Imaging Centre, Montreal Neurological Institute and Hospital, McGill University, Montreal, QC, Canada. Email: sjhong@bic.mni.mcgill.ca  [orcid.org/0000-0002-1847-578X](https://orcid.org/0000-0002-1847-578X)

## Abstract

In autism spectrum disorders (ASDs), the majority of neuroimaging studies have focused on the analysis of cortical morphology. White matter changes remain less understood, particularly their association to cortical structure and function. Here, we focused on region that has gained only little attention in ASD neuroimaging: the superficial white matter (SWM) immediately beneath the cortical interface, a compartment playing a prominent role in corticogenesis that incorporates long- and short-range fibers implicated in corticocortical connectivity. Studying a multicentric dataset of ASD and neurotypical controls, we harnessed surface-based techniques to aggregate microstructural SWM diffusion features. Multivariate analysis revealed SWM anomalies in ASD compared with controls in medial parietal and temporoparietal regions. Effects were similar in children and adolescents/adults and consistent across sites. Although SWM anomalies were more confined when correcting for cortical thickness and surface area, findings were overall robust. Diffusion anomalies modulated functional connectivity reductions in ASD and related to symptom severity. Furthermore, mediation models indicated a link between SWM changes, functional connectivity, and symptom load. Analyses targeting the SWM offer a novel perspective on the interplay between structural and functional network perturbations in ASD, highlighting a potentially important neurobiological substrate contributing to its diverse behavioral phenotype.

**Key words:** autism, connectome, neuroimaging, structure–function, white matter

## Introduction

Autism spectrum disorders (ASDs) are common and lifelong neurodevelopmental conditions characterized by atypical social cognition, communication, repetitive behaviors/interests, as well as sensory anomalies. While there are several histopathological reports of atypical cortical organization, neuronal migration, and white matter architecture (Avino and Hutsler 2010; Courchesne et al. 2011; Stoner et al. 2014), suggesting that ASD is associated with perturbations of different stages of corticogenesis, the brain basis of this condition remains elusive. Particularly, biological factors giving rise to its diverse

functional impairments and behavioral symptoms have been incompletely understood.

Neuroimaging, and in particular magnetic resonance imaging (MRI), lends a versatile window to study the brain at a macroscopic as well as microstructural level (Larivière et al. 2018) and to identify substrates of typical and atypical neurodevelopment. Using quantitative structural analyses, several studies mapped alterations in cortical morphology in children and adults with ASD relative to typically developing controls. Despite variability in the location of findings (Bernhardt, Di Martino, et al. 2017), studies show rather consistently cortical

thickening in ASD, particularly in frontal and temporal regions (Valk et al. 2015; Khundrakpam et al. 2017; van Rooij et al. 2018), decreases in surface area (Ecker et al. 2013; Hong et al. 2018), together with reduced intensity contrast along the cortical interface (Andrews et al. 2017; Hong et al. 2018). Collectively, these findings are indicative of perturbations in both vertical and horizontal cortical organization, potentially secondary to atypical corticogenesis and corticocortical network formation.

During neurodevelopment, the white matter emerges from the intermediate zone that is transiently located between the subventricular zone and cortical plate (Budday et al. 2015). Given its crucial role in supporting neuronal migration and in mediating connectivity between cortical areas, analysis of the white matter may provide a unique opportunity to track abnormal congenital processes in ASD, especially those occurring in corticocortical connectivity formation. The assessment of this compartment may also help contextualizing cortical morphological changes, given theoretical and empirical works suggesting an intricate interplay between white matter properties and cortical geometry in healthy individuals as well as those suffering from other neurodevelopmental conditions (White and Hilgetag 2011; Henderson and Robinson 2014). In ASD, recent studies leveraged diffusion-weighted imaging (DWI), a technique sensitive to regional tissue microstructure and fiber architecture through an analysis of water displacement properties (Beaulieu 2002; Jones et al. 2013; Jbabdi et al. 2015). Notably, DWI studies in ASD have focused mainly on deep fiber tracts, such as the corpus callosum and long-range fascicles (Travers et al. 2012; Aoki et al. 2013; Koldewyn et al. 2014). While supporting an association between ASD and alterations in white matter networks in vivo, the majority of DWI analyses has not directly examined the relation between white matter changes and neocortical morphology, except for a recent study suggesting an association between altered gyrification and structural connectivity (Ecker et al. 2016). Likewise, despite the overall assumption that structural connections largely determine functional dynamics (Honey et al. 2007), there have been no attempts to consolidate ASD-related changes in white matter integrity to cortical functional connectivity.

One region that has received only little attention in the neuroimaging of ASD is the superficial white matter (SWM), a compartment immediately beneath the cortical interface. In addition to its important role in genesis and maturation of the folded cortex (Toro and Burnod 2005; Herculano-Houzel et al. 2010), its spatial proximity ensures intrinsic correspondence to the cortical ribbon, making it an ideal candidate for integrative studies on cortical gray matter morphology, function, and white matter organization in ASD. Notably, as the SWM harbors both short- and long-range fibers mediating corticocortical connectivity (Parent and Carpenter 1996; Schüz and Braitenberg 2002; Oishi et al. 2008, 2011), likely contributing to functional network alterations and behavioral symptomatology in ASD. The current study investigated this so-far underrecognized zone based on a multicentric sample of individuals with ASD and typically developing controls. We harnessed multimodal image coregistration and postprocessing techniques for targeted surface placement and DWI parameter sampling within the SMW, allowing for the aggregation of in vivo markers of tissue microstructure and fiber architecture (Liu et al. 2016). Multivariate analysis synthesized spatial patterns of diffusion anomalies in this compartment in ASD relative to controls and established the relation to alterations in cortical morphology. To assess the link between SWM changes and those in cortical

function and behavior, we build correlative and mediation models to examine the interplay between changes in SWM diffusivity, functional connectivity, and symptom severity within our ASD group.

## Methods

### Subjects

Our study was based on a subsample from the Autism Brain Imaging Data Exchange II (ABIDE-II) dataset (Di Martino et al. 2017). Similar to previous studies (Hong et al. 2018), we selected those sites that contained children and adults ASD or typically developing controls and those for which DWI and T1-weighted data were available. Following automated cortical surface extraction and quality control (see “Quality control and inclusion criteria” in the following), our sample included 110 individuals from 3 sites: 1) NYU Langone Medical Center (NYU: 30 ASD, 19 controls); 2) Institut Pasteur and Robert Debré (IP: 12 ASD, 21 controls); 3) Trinity Center for Health Sciences (TCD: 11 ASD, 17 controls). While ASD and control subjects had comparable male/female ratios ( $P > 0.43$ ), they differed in age (ASD vs. controls mean  $\pm$  SD = 12.2  $\pm$  6.3 years vs. 16.7  $\pm$  8.3;  $P < 0.01$ ,  $t = 3.16$ ). Individuals with ASD had a DSM-V diagnosis of Autistic Disorder, Asperger’s Disorder, or Pervasive Developmental Disorder Not-Otherwise-Specified, established by the Autism Diagnostic Observation Schedule, ADOS (Lord et al. 2000), and/or the Autism Diagnostic Interview-Revised, ADI-R (Lord et al. 1994). For details on site-specific inclusion and exclusion criteria, see [http://fcon\\_1000.projects.nitrc.org/indi/abide/abide\\_II.html](http://fcon_1000.projects.nitrc.org/indi/abide/abide_II.html).

### MRI Acquisition

High-resolution T1-weighted images (T1w), diffusion-weighted images (DWI), and resting-state functional MRI (rs-fMRI) were available from all sites. NYU data were collected on a 3 T Siemens Magnetom Allegra scanner (T1w: TR = 2530 ms; TE = 3.25 ms; TI = 1100 ms; flip angle = 7°; axial slices = 128; matrix = 256  $\times$  192; FOV = 256 mm; slice thickness = 1.33 mm; voxels = 1.3  $\times$  1.0  $\times$  1.3 mm<sup>3</sup>; DWI: TR = 5200 ms; TE = 78 ms; flip angle = 60°; axial slices = 50; slice thickness = 3 mm; voxels = 3.0  $\times$  3.0  $\times$  3.0 mm<sup>3</sup>; directions = 64; b0 = 1000 s/mm<sup>2</sup>; rs-fMRI: 180 measurements; TR = 2000 ms; TE = 30 ms; flip angle = 82°; matrix = 80  $\times$  80; FOV = 240 mm; voxel size = 3.0  $\times$  3.0  $\times$  4.0 mm<sup>3</sup>). IP data were collected on a 1.5 T Phillips Achieva scanner (T1w: TR = 25 ms; TE = 5.6 ms; flip angle = 30°; axial slices = 170; matrix = 240  $\times$  240, slice thickness = 1.0 mm; FOV = 240 mm; voxels = 1.0  $\times$  1.0  $\times$  1.0 mm<sup>3</sup>; DWI: TR = 5407 mm; TE = 86 ms; flip angle = 90°; axial slices = 45; slice thickness = 2.5 mm; voxels = 2.50  $\times$  2.57  $\times$  2.50 mm<sup>3</sup>; directions = 32; b0 = 1000 s/mm<sup>2</sup>; rs-fMRI: 85 measurements; TR = 2700 ms; TE = 45 ms; flip angle = 90°; matrix = 64  $\times$  63; FOV = 230 mm; voxel size = 3.59  $\times$  3.65  $\times$  4.0 mm<sup>3</sup>). TCD data were acquired on a 3 T Philips Intera Achieva (T1w: TR = 8.4 ms; TE = 3.9 ms; TI = 1150 ms; matrix = 256  $\times$  256; FOV = 230 mm; slice thickness = 0.9 mm; flip angle = 8°; voxels = 0.9  $\times$  0.9  $\times$  0.9 mm<sup>3</sup>; DWI: TR = 20 244 ms; TE = 79 ms; matrix = 124  $\times$  124; FOV = 248; slice thickness = 2 mm; flip angle = 90° voxels = 1.94  $\times$  1.94  $\times$  2.0 mm<sup>3</sup>; directions = 61; b0 = 1500 s/mm<sup>2</sup>; rs-fMRI: 210 measurements; TR = 2000 ms; TE = 27; matrix = 80  $\times$  80; FOV = 240; slice thickness = 3.2 mm; flip angle = 90° voxels = 3  $\times$  3  $\times$  3.2 mm<sup>3</sup>).

## MRI Preprocessing

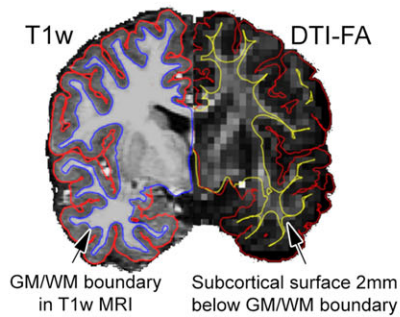
a. Structural MRI. We used FreeSurfer (v5.3; <https://surfer.nmr.mgh.harvard.edu/fswiki>) for T1w MRI processing, with details described elsewhere (Dale et al. 1999; Fischl, Sereno and Dale 1999; Fischl, Sereno, Tootell, et al. 1999; Fischl and Dale 2000). In brief, FreeSurfer automatically reconstructed geometric models approximating the inner and outer cortical interfaces based on a series of volume- and surface-based processing steps. Following surface extraction, individual surfaces were registered to fsaverage5, a group-level

template with 20 484 surface points, via alignment of cortical folding patterns. Surface extractions were visually inspected, and segmentation inaccuracies manually corrected by a rater blind to diagnostic category (BH).

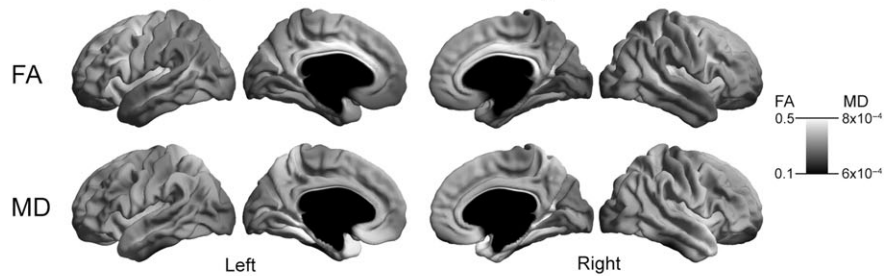
b. DWI. Processing was based on MRtrix<sup>3</sup> (v0.3.15; <http://www.mrtrix.org/>) and involved correction for head motion and eddy currents as well as estimation of diffusion parameters, that is, fractional anisotropy (FA) and mean diffusivity (MD). Preprocessed data were visually inspected by one rater blind to diagnosis (BH), and subjects with no or faulty DWI data were removed. Each subject's white matter boundary

## A SWM analysis

### Surface generation

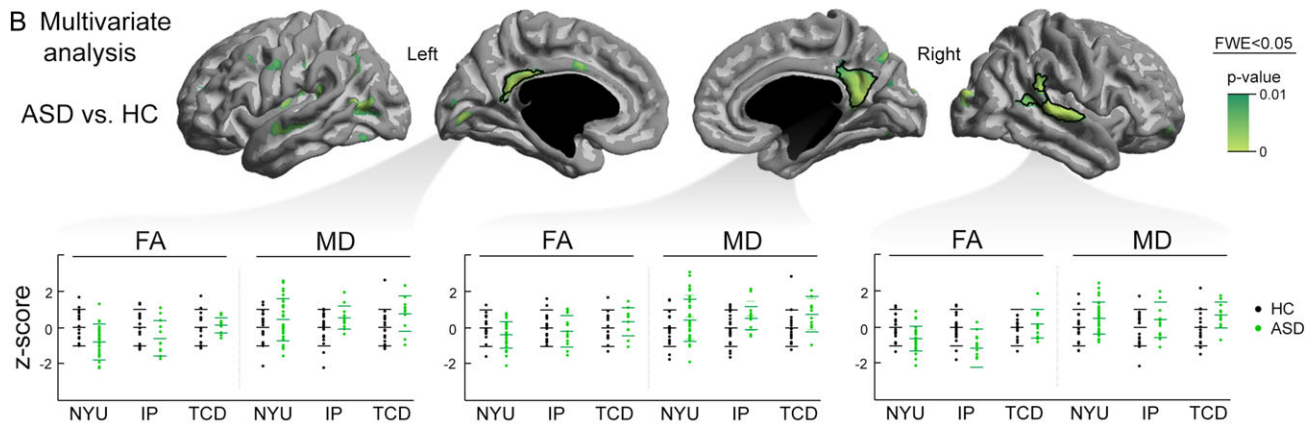


### DTI indices of superficial white matter in healthy controls



## B Multivariate analysis

### ASD vs. HC



## C Univariate analysis

### FA ASD vs. HC

### MD ASD vs. HC

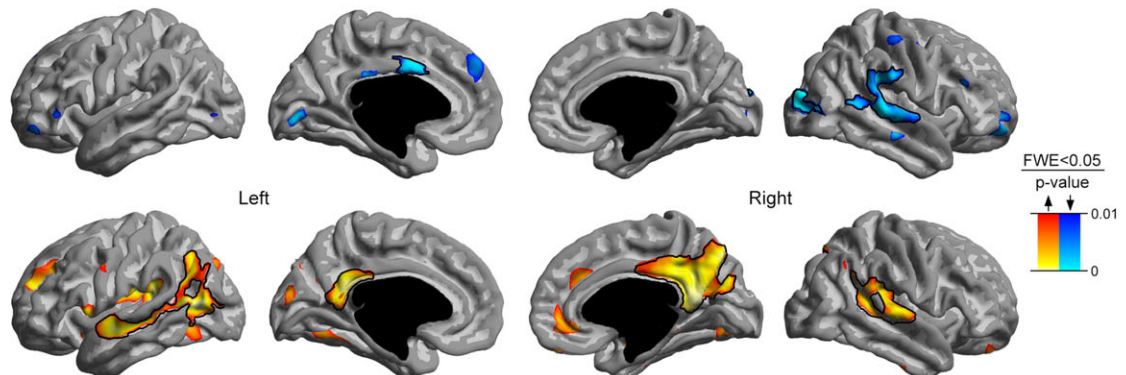


**Figure 1.** (A) To sample diffusion parameters in the SWM, we propagated the inner cortical boundary inward along a Laplacian potential field toward the ventricles (Left panel). Group-averaged SWM-FA and -MD maps in typically developing controls are shown (Right panel). (B) Multivariate comparisons on overall SWM diffusion anomalies (aggregating in FA and MD) in ASD compared with controls. Post hoc analysis in clusters of findings supported consistency across the included sites (i.e., NYU, IP, TCD), characterized by increased MD and reduced FA. (C) Surface-wide univariate analysis, showing marked and bilateral MD changes and more restricted FA anomalies. Findings with black outlines were corrected for multiple comparisons. Uncorrected trends are superimposed in semitransparent.



derived from T1w MRI was coregistered to the DWI b0 image using a boundary-based registration by maximizing the intensity difference at the cortical interface (Greve and Fischl 2009).

- c. rs-fMRI. Processing procedures were based on the Pre-processed Connectomes initiative (<http://preprocessed-connectomes-project.org/abide/>) and used C-PAC (<https://fcp-indi.github.io/>). Procedures included slice-time correction, head motion correction, skull stripping, and intensity normalization. Statistical corrections removed effects of head motion (Friston et al. 1996), white matter and cerebrospinal fluid signals [using “CompCor,” based on the top 5 principal components (Behzadi et al. 2007)], as well as linear/quadratic trends. After band-pass filtering (0.01–0.1 Hz), we coregistered rs-fMRI and T1w data in MNI152 space through combined linear and nonlinear transformations. Surface alignment was verified for each case and we interpolated voxel-wise rs-fMRI time series along mid-thickness surfaces. We resampled rs-fMRI surface data to fsaverage5 and applied surface-based smoothing. For each subject, we performed a visual scoring of surface extractions for structural MRI and evaluated temporal derivatives and frame-wise displacement metrics for rs-fMRI (Jenkinson et al. 2002; Power et al. 2012).

### Quality Control and Inclusion Criteria

Across the 3 sites, a total of 143 subjects had T1w and DWI images (including bvecs and bvals) available. We excluded 21 cases based on data quality (e.g., head motion, low T1w tissue contrast, artifacts on DWI data). Coregistrations of individual SWM surfaces to DWI space were visually inspected, leading to further exclusion of 12 participants with poor alignment. Our final cohort, thus, consisted of 110 total participants: 53 ASD (age:  $12.2 \pm 6.3$  years, 45 males) and 57 typically developing controls (age:  $16.7 \pm 8.3$  years, 44 males).

### Surface-based Feature Generation

- a. SWM surface generation and diffusion parameter sampling. As in previous studies in drug-resistant epilepsy and healthy controls (Liu et al. 2016; Valk et al. 2016), we computed a Laplacian potential field between the white–gray matter interface and the ventricular walls to guide placement of a SWM surface running approximately 2 mm below the gray/white matter boundary (Fig. 1A). This depth was chosen to target both the U-fiber system and terminations of long-range bundles that lie between 1.5–2.5 mm below the cortical interface (Schüz and Braitenberg 2002). The Laplacian field ensured an isomorphic mapping between points on the SWM surface and those on the overlying cortex, allowing for seamless integration of gray and white matter metrics. SWM surfaces were mapped to DWI space using previously estimated coregistrations. Voxel-wise FA and MD values were interpolated to all surface points along this newly mapped SWM surface. Measurements were registered to fsaverage5 and smoothed using a 20-mm full-width-at-half-maximum (FWHM) surface-diffusion kernel. Unlike voxel-based isotropic smoothing, kernels operating within the cortical manifold reduce measurement noise while respecting cortical anatomy (Chung et al. 2001; Lerch 2005).
- b. Cortical morphological parameterization. We measured “cortical thickness” as the distance of corresponding vertices

between the inner and outer cortical interfaces. As for SWM parameters, we resampled thickness to fsaverage5 and smoothed measures via 20-mm FWHM kernels. Along the white matter interface, we also measured average “surface area” of the 6 triangles surrounding a given vertex. To account for interpolation effects during surface registration (Winkler et al. 2012), we computed this metric on surfaces already resampled to fsaverage5. As for the other markers, surface area was smoothed using with a 20-mm FWHM kernel.

### Multimodal Analyses

As in previous work (Bernhardt, Bernasconi, et al. 2016; Hong et al. 2016), analyses were carried out in SurfStat (Worsley et al. 2009) for Matlab (2017; The Mathworks).

- a. Analysis of SWM diffusivity. Multivariate linear models at each cortical surface point  $i$  assessed the differences in a multivariate aggregate  $MV_i$ , based on FA and MD between ASD and controls.

$$MV_i = \beta_0 + \beta_1 * \text{Sex} + \beta_2 * \text{Age} + \beta_3 * \text{Site} + \beta_4 * \text{Motion} + \beta_5 * \text{Group}$$

Models corrected for “Sex” and “Age” given their effects on brain morphology and diffusion properties (Phillips et al. 2013; Ritchie et al. 2018), “Site” to account for systematic differences in acquisition parameters, and average root-mean-square displacement of each DWI volume compared with the previous one as an index of head motion (Taylor et al. 2016; Baum et al. 2018). Parallel univariate models evaluated between-group differences in FA and MD.

- b. Assessment of cortical morphology. We evaluated differences in cortical thickness and surface area between ASD and controls using linear models. As in the diffusion parameter analysis, models testing for differences in cortical thickness controlled for “Sex,” “Age,” and “Site.”

$$CT_i = \beta_0 + \beta_1 * \text{Sex} + \beta_2 * \text{Age} + \beta_3 * \text{Site} + \beta_4 * \text{Group}$$

In keeping with recent ASD studies (Ecker et al. 2013; Hong et al. 2018), the model testing for differences in surface area additionally controlled for “Total White Matter Volume.”

$$SA_i = \beta_0 + \beta_1 * \text{Sex} + \beta_2 * \text{Age} + \beta_3 * \text{Site} + \beta_4 * \text{Group} + \beta_5 * \text{WMVOL}$$

- c. Controlling for variations in cortical morphology. To account for morphological variability in diffusion parameter comparisons, we corrected for “Cortical Thickness” and “Surface Area” at each surface point and repeated the above models on the residual SWM data.
- d. Relationship to functional connectivity and symptom severity. We carried out a series of post hoc functional connectivity analyses (focusing on those clusters showing DWI alterations in ASD compared with controls, see a). Each cluster’s functional connectivity was calculated as Pearson’s correlation coefficient between the average time series of the cluster and time series of every other cortical vertex. Fisher  $r$ -to- $z$  transformations rendered correlation coefficients more normally distributed. For each cluster, we ran surface-wide linear models that compared its connectivity strength between ASD and controls, controlling for age, sex, site, and

mean framewise displacement to account for head motion (Power et al. 2012). Within ASD, we correlated interindividual differences of SWM anomalies with individual differences in functional connectivity (i.e., z-scored functional connectivity, relative to controls), to examine whether ASD individuals with more severe SWM alterations also displayed more marked functional connectivity changes. To capture overall ASD-related SWM anomalies, we built a single composite score that captured the degree of FA decreases and MD increases in single subjects. To this end, we calculated the mean of the average z-scored FA reduction and z-scored MD increase in clusters of significant diffusion MRI findings, both relative to healthy controls. To furthermore examine associations to behavioral symptoms of ASD, we correlated interindividual differences in SWM measures with ADOS scores in ASD and finally built path analytical models using a freely released Matlab toolbox (<https://github.com/canlab/MediationToolbox>), evaluating the role of functional connectivity on the relation between diffusion anomalies and ADOS scores.

- e. Correction for multiple comparisons. Surface-based analyses were corrected using random-field theory for nonisotropic images (Worsley et al. 1999) with a threshold of familywise error of  $P_{FWE} < 0.05$  (cluster defining threshold,  $CDT = 0.01$ ).

### Data Availability

All data used in this study are openly shared via FCP/INDI, with further information on the included sites found at [http://fcon\\_1000.projects.nitrc.org/indi/abide/abide\\_II.html](http://fcon_1000.projects.nitrc.org/indi/abide/abide_II.html).

## Results

### SWM Diffusion Anomalies

Multivariate diffusion parameter analysis mapped a high load of SWM anomalies in ASD compared with controls ( $P_{FWE} < 0.05$ ; Fig. 1B) in bilateral medial parietal cortices encompassing precuneus and posterior cingulate (PCU-PCC) as well as the right temporoparietal junction (TPJ).

Post hoc analysis in clusters confirmed similar effect sizes across the 3 included sites (FA Cohen's  $d = 0.76/0.74/0.32$ , MD  $d = 0.53/0.67/0.83$  [NYU/IP/TCD]; Fig. 1B). Separately analyzing children (age < 12.5 [median]) and adolescents/adults (age  $\geq 12.5$ ) revealed comparable effects (children: FA/MD  $d = 0.54/0.67$ ; adolescents/adults: FA/MD  $d = 0.65/0.59$ ), indicating consistent SWM diffusion changes across age groups. Diffusion anomalies in all clusters were typified by reduced FA (left/right PCU-PCC  $d = 0.2/0.48$ , right TPJ  $d = 0.74$ ) and increased MD (left/right PCU-PCC  $d = 0.72/0.65$ , right TPJ  $d = 0.61$ ) in ASD. Univariate analysis (Fig. 1C) indicated that MD findings were more widespread, including bilateral medial parietal and temporoparietal regions, while FA changes appeared restricted to the right TPJ. In a separate analysis, we also assessed axial and radial diffusivity (Supplementary Fig. 1); across all clusters, ASD showed consistent increases in radial diffusivity compared with controls while the right PCC additionally revealed increased axial diffusivity.

### Relation to Cortical Morphology

We mapped surface-wide changes in cortical thickness and surface area in ASD relative to controls (Fig. 2A). Although of no significant differences in both parameters after correction for multiple comparisons, we observed tendencies for cortical

thickening in temporolimbic and medial frontal areas ( $P < 0.025$ ), in keeping with earlier reports on ABIDE subsamples and recent meta-analyses (Valk et al. 2015; Khundrakpam et al. 2017; van Rooij et al. 2017).

Furthermore, we observed tendencies of decreases in surface areas in prefrontal, insular, and temporal regions, also confirming earlier findings (Ecker et al. 2013; Hong et al. 2018). Importantly, although the extent of SWM anomalies in ASD compared with controls was reduced after controlling for cortical thickness and surface area at each cortical vertex (Fig. 2B), effects in right hemisphere clusters persisted after correcting for morphological variations, specifically in the PCC/PCU and TPJ clusters.

### Relation to Functional Connectivity and Behavioral Symptoms

To explore functional associations, we carried out a seed-based resting-state functional connectivity analyses from clusters of multivariate SWM anomalies (Fig. 3A). In controls (Fig. 3B), PCC-PCU clusters were closely integrated into the DMN, showing high functional connectivity to bilateral medial frontal and parietal regions, as well as superior temporal and angular cortices. Seeding from the right TPJ, on the other hand, we observed connections to other temporal, cingulate, midline parietal, and insular regions.

Statistically comparing ASD with controls (Fig. 3C) revealed connectivity reductions in the former, with left PCC-PCU disconnected from more distant targets in prefrontal and premotor areas, while right PCC-PCU showed connectivity reductions to the adjacent cuneus. Right TPJ regions also showed reductions in functional connectivity to proximal cortical areas, notably posterior insular and superior parietal cortices. As for the diffusion parameter findings, connectivity reductions were consistent across sites (Fig. 3D).

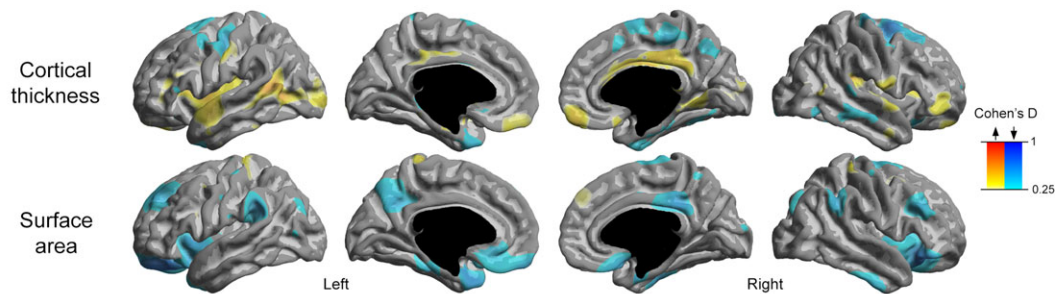
In the ASD group, interindividual differences in SWM anomalies in both right hemispheric clusters correlated with the overall degree of functional connectivity reductions to those target areas (i.e., adjacent cuneus, and the posterior insular and superior parietal cortices). In other words, individuals with ASD who showed more marked SWM anomalies (defined by multivariate composite scores of FA and MD) also displayed more marked reductions in functional connectivity ( $SWM_{TPJ}$ :  $r = -0.38$ ,  $P < 0.0025$ ;  $SWM_{PCC/PCU}$ :  $r = -0.25$ ,  $P < 0.037$ , Fig. 3E).

Overall SWM profile (averaged score of  $SWM_{TPJ}$  and  $SWM_{PCC/PCU}$ ) was also associated to more severe ASD symptoms, as indexed by total ADOS ( $r = 0.27$ ,  $P < 0.04$ ). Separate univariate analyses suggested that results were mainly driven by FA ( $r = -0.24$ ,  $P = 0.054$ ), not MD ( $P > 0.4$ ). Finally, correlations between SWM anomalies and total ADOS scores were found to be partially mediated by reduced functional connectivity ( $z = 1.93$ ,  $P < 0.06$ ), suggesting a disease-related path between SWM alterations, functional connectivity reductions, and behavioral symptoms (Fig. 4). Separate assessments on specific ADOS scores revealed that the observed mediation was mainly attributable to the social cognition domain (mediation effect:  $z = 1.84$ ,  $P < 0.07$  for social cognition;  $P > 0.1$  for communication and repeated behavior domains).

## Discussion

The current work targeted the SWM, the so-far largely neglected compartment in autism based on multimodal in vivo imaging. Our surface-based analyses of different diffusion MRI

## A Group comparison of cortical morphology



## B Morphology-corrected superficial white matter analysis

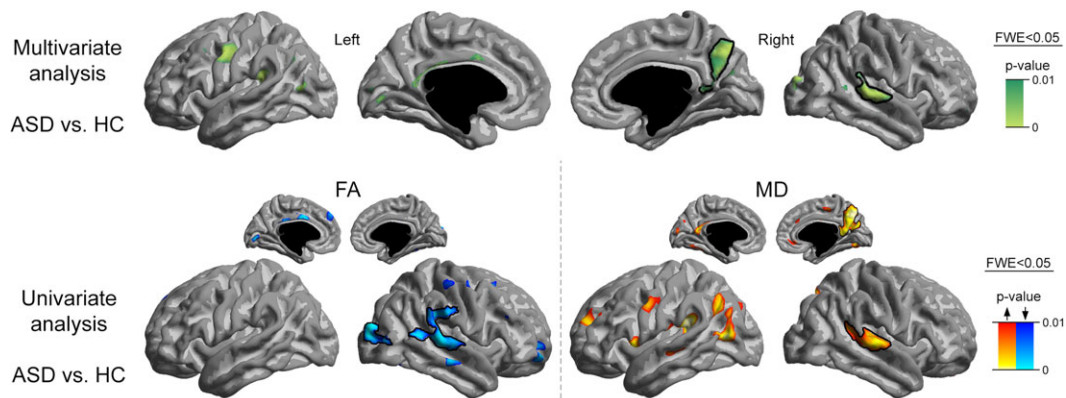


**Figure 2.** (A) Alterations in cortical morphology (cortical thickness and surface area) in ASD compared with controls. (B) Persistence of SWM diffusion anomalies after correcting for cortical thickness and surface area at each vertex. For details on the statistical thresholds, see Figure 1.

parameters in a multicentric dataset of ASD and typically developing controls revealed atypical SWM organization in medial parietal and lateral posterior temporal regions in ASD. Analysis across different sites indicated high consistency of findings, as did separate assessments in children, adolescents, and adults. Although the extent of findings was slightly reduced after correcting for MRI-derived cortical thickness and surface areas, anomalies remained largely robust against correction for morphological variations. The pattern of SWM changes observed in the current study may thus indicate partially overlapping, yet also distinct developmental perturbations as those affecting vertical and horizontal cortical morphological organization. Assessing coregistered resting-state fMRI data at an interindividual level, we also observed that SWM findings correlated with intrinsic functional connectivity changes, supporting a potential contribution to previously reported functional network alterations in ASD. Finally, SWM changes parametrically related to ADOS symptom load, and this effect was found to be mediated by functional anomalies, suggesting that SWM anomalies may serve as a potential substrate of atypical functional connectome organization and the phenotypic expression of ASD.

Immediately subjacent to the cortical ribbon and serving as a corridor for neuronal migration during development, the SWM represents an important candidate area to assess effects of typical and atypical cortical organization and corticocortical network formation. Its pivotal role in cortical connectivity is indeed reflected in the SWM harboring both short-range association fibers, such as the U-fiber system arching through the cortical sulci to connect adjacent gyral regions, as well as

termination fibers of long-range tracts running throughout the deep white matter (Schüz and Braitenberg 2002; Vergani et al. 2014). Interestingly, while its overall components are already fully formed throughout the prenatal corticogenic phase, large-scale changes still occur in the SWM even after birth. In fact, this compartment is thought to show marked and protracted changes in connectivity and myelination patterns both for long-range corticosubcortical projection and short-range U-fiber networks in the first years of life (Parazzini et al. 2002), possibly to support the parallel emergence and maturation of functional systems. Indeed, the SWM has increasingly been recognized to contribute to multiple perceptual and higher level cognitive abilities, ranging from sensory and attentional function (Nazeri et al. 2015) to social and meta-cognitive awareness (Valk et al. 2016). Notably, despite the absence of neuroimaging work on this compartment in ASD, changes in the SWM have recently been highlighted in studies focusing on childhood neurodevelopment (Wu et al. 2014), aging (Phillips et al. 2013), and prevalent disorders associated with aberrant corticogenesis, including temporal lobe epilepsy (Liu et al. 2016) and malformations of cortical development (Hong et al. 2017).

Comparing ASD with controls, we observed SWM diffusion anomalies in the former group, characterized by increased MD together with FA reductions in medial parietal and lateral temporoparietal regions. Findings were consistent across the 3 included sites albeit variable effect sizes in each of them. Although lack of additional histopathological and quantitative MRI markers renders specific microstructural and architectural interpretations difficult, post hoc analysis revealed mainly increased radial diffusivity (i.e., a diffusion degree along non-



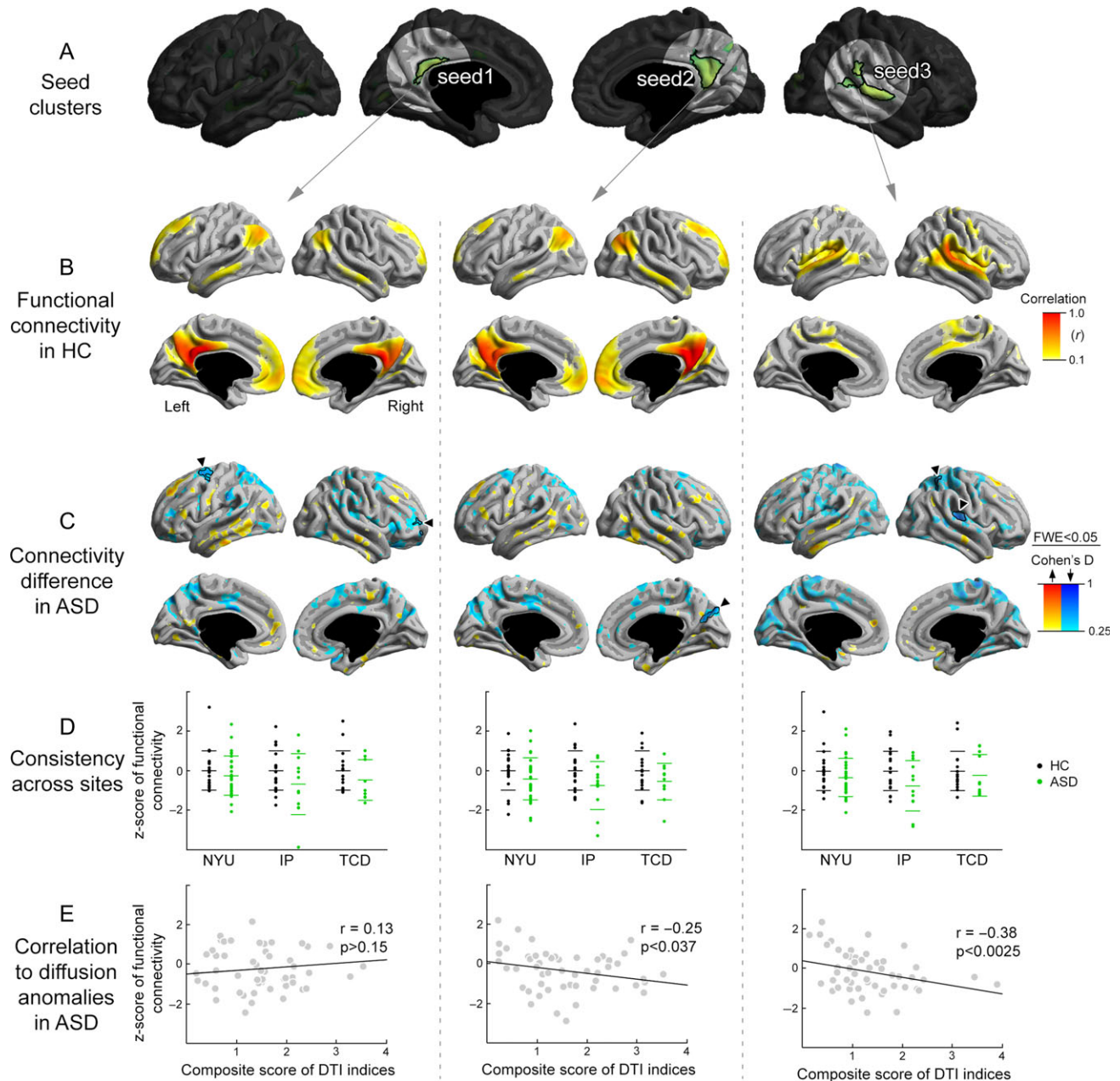


**Figure 3.** (A) Seed clusters for functional connectivity. (B) Functional connectivity maps in healthy controls (HC). (C) Surface-based differences in seed-based functional connectivity in ASD versus controls. (D) Consistency of effect across the 3 included sites. (E) Post hoc correlations between SWM diffusion changes and average functional connectivity reductions.

primary directions) across significant clusters, a pattern of findings compatible with reductions in fiber packing and demyelination together with increases in extracellular space (Alexander et al. 2007). This is supported by effects that were, while generally robust when correcting for morphological variations, somewhat diminished when cortical thickness and surface area were statistically controlled for. A plausible factor in the partial interaction between cortex morphology and SWM alterations may be the overall number of connections a given cortical region with a predefined thickness and surface area can emit and receive. This finding would also be in line with recent reports on coupled mechanisms affecting deep WM connectivity and cortical shape complexity in ASD (Schaer et al. 2013;

Ecker et al. 2016). Furthermore, they complement histological data showing reductions in long-range axons with co-occurring increases in short-range connections in ASD (Zikopoulos and Barbas 2010, 2013).

Advances in resting-state fMRI methodologies have resulted in a surge of studies assessing functional network anomalies in ASD relative to neurotypical cohorts, contributing to the notion that autism may be associated to a “miswired connectome” (Di Martino, Fair, et al. 2014). Despite little consensus in location of findings and direction of changes (Uddin et al. 2010; Deen and Pelphrey 2012; Keown et al. 2013; Yahata et al. 2016; Heinsfeld et al. 2018; Larivière et al. 2018), the literature generally suggests a predominance of reductions in corticocortical

## Behavioral correlation and mediation analysis

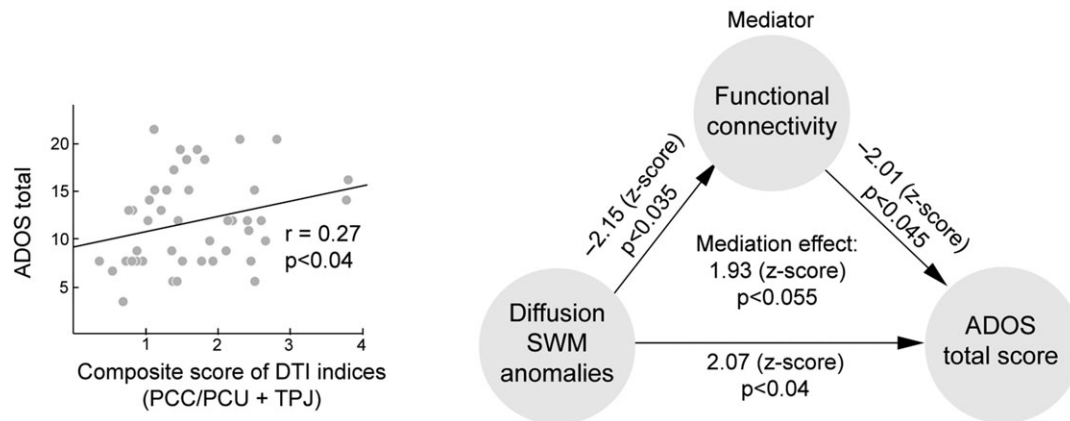


**Figure 4.** Correlation between SWM diffusion anomalies and total ADOS scores (left). Functional connectivity was found to mediate the relation between diffusion anomalies and ADOS scores (right)

connectivity in ASD. This is particularly the case for transmodal regions participating in high-level cognitive and social processes, notably default mode network core regions in medial parietal and the lateral temporal/temporoparietal cortices (Di Martino, Yan, et al. 2014), that is, those regions highlighted by our fully unconstrained and surface-wide DWI analysis. Post hoc analyses from clusters of significant SWM diffusion anomalies confirmed functional connectivity reductions in ASD relative controls across all of them. Furthermore, and beyond the colocalization of structural and functional connectivity anomalies, we observed an association between the degree of SWM anomalies and those in intrinsic functional connectivity in ASD, specifically in right hemisphere seeds, suggesting that SWM changes may represent an important substrate of interindividual differences in the perturbation of corticocortical functional interactions. Notably, connectivity reductions did not seem to follow a specific anatomical distance distribution, suggesting that functional decoupling may affect both short- and long-range components of the corticocortical resting-state fMRI connectome.

The loco-regional network effects seen in the SWM might have important implications for cortical information processing in ASD. Correlating SWM changes to ADOS scores, we could indeed gather evidence for an association between diffusion anomalies in the subjacent white matter and overall symptom severity. Furthermore, associations were found to be partially mediated by fMRI anomalies, indicating that functional connectivity perturbations downstream to the SWM changes might indeed have contributed to this association. The associations with total symptom scores were mainly driven by the sociocognitive subscale of the ADOS, overall in agreement with the implication of PCC/PCU and TPJ (i.e., those areas showing diffusion anomalies correlated to ADOS) in sociocognitive processes related to “theory of mind” and more generally cognitive perspective taking in neurotypical cohorts and ASD. Indeed, task-based fMRI studies have shown a rather consistent involvement of midline parietal and lateral temporoparietal areas during mentalizing tasks in typically developing children and adults (Saxe and Kanwisher 2003; Mitchell et al. 2006; Van Overwalle 2009; Mar 2011; Bzdok et al. 2012; Gweon et al. 2012; Schurz et al. 2014), suggesting a contribution of these areas to sociocognitive functioning. Such findings have been complemented by morphometric and MRI covariance data supporting

a relationship between these regions’ morphology and interregional structural network embedding on the one hand, and phenotypic variations in social cognitive functions on the other hand (Valk et al. 2016; Valk, Bernhardt, Bockler, et al. 2017; Valk, Bernhardt, Trautwein, et al. 2017). In line with the longstanding association of ASD to “atypical theory of mind” (Frith and Frith 2005), task-based fMRI in the condition revealed atypical activations during cognitive perspective-taking tasks in these regions (Castelli et al. 2002; Kennedy and Courchesne 2008; Kana et al. 2009; Lombardo et al. 2011). Moreover, resting-state findings have supported rather consistent connectivity perturbations of midline parietal (Di Martino, Yan, et al. 2014; Joshi et al. 2017) and temporoparietal areas in ASD (Uddin et al. 2013). Together with structural covariance findings indicating anomalies in the large-scale morphological coordination (Bernhardt et al. 2014), these results collectively support a disrupted structure–function network embedding of these regions in ASD.

We close by noting that our work also provides practical insight that surface-based SWM profiling information can be easily integrated with widely used markers of cortical morphology and functional connectivity. As our findings have shown in ASD, microstructural and architectural organization of the SWM may overall contribute to large-scale cortical function and behavioral symptoms in neurodevelopmental conditions. In other neurological or psychiatric disorders such as epilepsy (Liu et al. 2016), Huntington’s disease (Phillips, Joshi, Squitieri, et al. 2016), Alzheimer’s disease (Phillips, Joshi, Piras, et al. 2016), psychosis (Makowski et al. 2018), and schizophrenia (Zhuo et al. 2016), similar analyses discovered functionally relevant structural compromise in the SWM, unveiling both common and distinct patterns of their tissue anomalies. Given the increasing availability of large transdiagnostic samples such as the healthy brain network (Alexander et al. 2017) and recent initiatives to transcend traditional diagnostic categories (Insel 2014), further studies are recommended that assess specificity of our findings for ASD and that clarify commonalities across disorders.

### Supplementary Material

Supplementary material is available at *Cerebral Cortex* online.



## Funding

The NYU site was supported by NIH (R21MH102660; K23MH087770; R21MH084126; R01MH081218; R01HD065282), the Stavros Niarchos Foundation, the Leon Levy Foundation, Phyllis Green and Randolph Cowen, and Goldman Sachs Gives. The IP site was supported by the Institut Pasteur, CNRS, INSERM, AP-HP, University Paris 7 Diderot, the BioPhys Labex, the DHU PROTECT, the Bettencourt-Schueller Foundation, the FondaMental Foundation, and the ANR. Dr S.-J.H. was supported by a fellowship from the Canadian Institutes of Health Research (CIHR). Dr C.P. is grateful for a postdoctoral fellowship by the transforming autism care consortium (TACC). Dr B.C.B. acknowledges research support from the National Science and Engineering Research Council of Canada (NSERC, Discovery-1304413), Canadian Institutes of Health Research (CIHR, FDN-154298), Azrieli Center for Autism Research, SickKids Foundation (NI17-039), as well as salary support from the Fonds de la Recherche du Québec—Santé (FRQS, Chercheur Boursier Junior 1).

## Notes

The authors thank the contributors at each site ([http://fcon\\_1000.projects.nitrc.org/indi/abide/](http://fcon_1000.projects.nitrc.org/indi/abide/)) and the NeuroImaging Tools & Resources Collaboratory (<http://www.nitrc.org>) for providing the data for the ABIDE-II initiative. *Conflict of Interest:* None declared.

## References

- Alexander LM, Escalera J, Ai L, Andreotti C, Febre K, Mangone A, Vega-Potler N, Langer N, Alexander A, Kovacs M, et al. 2017. An open resource for transdiagnostic research in pediatric mental health and learning disorders. *Scientific Data*. 4: 170181.
- Alexander AL, Lee JE, Lazar M, Field AS. 2007. Diffusion tensor imaging of the brain. *Neurotherapeutics*. 4:316–329.
- Andrews DS, Avino TA, Gudbrandson M, Daly E, Marquand A, Murphy CM, Lai MC, Lombardo MV, Ruigrok AN, Williams SC, et al. 2017. In vivo evidence of reduced integrity of the gray-white matter boundary in autism spectrum disorder. *Cereb Cortex*. 27:877.
- Aoki Y, Abe O, Nippashi Y, Yamasue H. 2013. Comparison of white matter integrity between autism spectrum disorder subjects and typically developing individuals: a meta-analysis of diffusion tensor imaging tractography studies. *Molecular Autism*. 4:25.
- Avino TA, Hutsler JJ. 2010. Abnormal cell patterning at the cortical gray-white matter boundary in autism spectrum disorders. *Brain Res*. 1360:138–146.
- Baum GL, Roalf DR, Cook PA, Ciric R, Rosen AFG, Xia C, Elliott MA, Ruparel K, Verma R, Tunc B, et al. 2018. The impact of in-scanner head motion on structural connectivity derived from diffusion MRI. *Neuroimage*. 173:275–286.
- Beaulieu C. 2002. The basis of anisotropic water diffusion in the nervous system—a technical review. *NMR Biomed*. 15: 435–455.
- Behzadi Y, Restom K, Liu J, Liu TT. 2007. A component based noise correction method (CompCor) for BOLD and perfusion based fMRI. *Neuroimage*. 37:90–101.
- Bernhardt BC, Bernasconi A, Liu M, Hong SJ, Caldairou B, Goubran M, Guiot MC, Hall J, Bernasconi N. 2016. The spectrum of structural and functional imaging abnormalities in temporal lobe epilepsy. *Ann Neurol*. 80:142–153.
- Bernhardt BC, Di Martino A, Valk SL, Wallace GL. 2017. Neuroimaging-Based Phenotyping of the Autism Spectrum. *Curr Top Behav Neurosci*. 30:341–355.
- Bernhardt BC, Valk SL, Silani G, Bird G, Frith U, Singer T. 2014. Selective Disruption of sociocognitive structural brain networks in autism and alexithymia. *Cereb Cortex*. 24: 3258–3267.
- Budday S, Steinmann P, Kuhl E. 2015. Physical biology of human brain development. *Front Cell Neurosci*. 9:257.
- Bzdok D, Schilbach L, Vogeley K, Schneider K, Laird AR, Langner R, Eickhoff SB. 2012. Parsing the neural correlates of moral cognition: ALE meta-analysis on morality, theory of mind, and empathy. *Brain Struct Funct*. 217:783–796.
- Castelli F, Frith C, Happe F, Frith U. 2002. Autism, Asperger syndrome and brain mechanisms for the attribution of mental states to animated shapes. *Brain*. 125:1839–1849.
- Chung MK, Worsley KJ, Taylor J, Ramsay J, Robbins S, Evans AC. 2001. Diffusion smoothing on the cortical surface. *Neuroimage*. 13:S95–S95.
- Courchesne E, Mouton PR, Calhoun ME, Semendeferi K, Ahrens-Barbeau C, Hallett MJ, Barnes CC, Pierce K. 2011. Neuron number and size in prefrontal cortex of children with autism. *JAMA*. 306:2001–2010.
- Dale AM, Fischl B, Sereno MI. 1999. Cortical surface-based analysis. I. Segmentation and surface reconstruction. *Neuroimage*. 9:179–194.
- Deen B, Pelphrey K. 2012. Perspective: brain scans need a rethink. *Nature*. 491:S20.
- Di Martino A, Fair DA, Kelly C, Satterthwaite TD, Castellanos FX, Thomason ME, Craddock RC, Luna B, Leventhal BL, Zuo XN, et al. 2014. Unraveling the miswired connectome: a developmental perspective. *Neuron*. 83:1335–1353.
- Di Martino A, O'Connor D, Chen B, Alaerts K, Anderson JS, Assaf M, Balsters JH, Baxter L, Beggiato A, Bernaerts S, et al. 2017. Enhancing studies of the connectome in autism using the autism brain imaging data exchange II. *Sci Data*. 4: 170010.
- Di Martino A, Yan CG, Li Q, Denio E, Castellanos FX, Alaerts K, Anderson JS, Assaf M, Bookheimer SY, Dapretto M, et al. 2014. The autism brain imaging data exchange: towards a large-scale evaluation of the intrinsic brain architecture in autism. *Mol Psychiatry*. 19:659–667.
- Ecker C, Andrews D, Dell'Acqua F, Daly E, Murphy C, Catani M, Thiebaut de Schotten M, Baron-Cohen S, Lai MC, Lombardo MV, et al. 2016. Relationship between cortical gyrification, white matter connectivity, and autism spectrum disorder. *Cereb Cortex*. 26:3297–3309.
- Ecker C, Ginestet C, Feng Y, Johnston P, Lombardo MV, Lai MC, Suckling J, Palaniyappan L, Daly E, Murphy CM, et al. 2013. Brain surface anatomy in adults with autism: the relationship between surface area, cortical thickness, and autistic symptoms. *JAMA Psychiatry*. 70:59–70.
- Fischl B, Dale AM. 2000. Measuring the thickness of the human cerebral cortex from magnetic resonance images. *Proc Natl Acad Sci U S A*. 97:11050–11055.
- Fischl B, Sereno MI, Dale AM. 1999. Cortical surface-based analysis. II: inflation, flattening, and a surface-based coordinate system. *Neuroimage*. 9:195–207.
- Fischl B, Sereno MI, Tootell RB, Dale AM. 1999. High-resolution intersubject averaging and a coordinate system for the cortical surface. *Hum Brain Mapp*. 8:272–284.
- Friston KJ, Williams S, Howard R, Frackowiak RS, Turner R. 1996. Movement-related effects in fMRI time-series. *Magn Reson Med*. 35:346–355.

- Frith C, Frith U. 2005. Theory of mind. *Curr Biol.* 15:R644–R646.
- Greve DN, Fischl B. 2009. Accurate and robust brain image alignment using boundary-based registration. *Neuroimage.* 48:63–72.
- Gweon H, Dodell-Feder D, Bedny M, Saxe R. 2012. Theory of mind performance in children correlates with functional specialization of a brain region for thinking about thoughts. *Child Dev.* 83:1853–1868.
- Heinsfeld AS, Franco AR, Craddock RC, Buchweitz A, Meneguzzi F. 2018. Identification of autism spectrum disorder using deep learning and the ABIDE dataset. *Neuroimage Clin.* 17: 16–23.
- Henderson JA, Robinson PA. 2014. Relations between the geometry of cortical gyrification and white-matter network architecture. *Brain Connectivity.* 4:112–130.
- Herculano-Houzel S, Mota B, Wong P, Kaas JH. 2010. Connectivity-driven white matter scaling and folding in primate cerebral cortex. *Proc Natl Acad Sci U S A.* 107: 19008–19013.
- Honey CJ, Kotter R, Breakspear M, Sporns O. 2007. Network structure of cerebral cortex shapes functional connectivity on multiple time scales. *Proc Natl Acad Sci U S A.* 104: 10240–10245.
- Hong SJ, Bernhardt BC, Caldaïrou B, Hall JA, Guiot MC, Schrader D, Bernasconi N, Bernasconi A. 2017. Multimodal MRI profiling of focal cortical dysplasia type II. *Neurology.* 88:734–742.
- Hong SJ, Bernhardt BC, Schrader DS, Bernasconi N, Bernasconi A. 2016. Whole-brain MRI phenotyping in dysplasia-related frontal lobe epilepsy. *Neurology.* 86:643–650.
- Hong SJ, Valk SL, Di Martino A, Milham MP, Bernhardt BC. 2018. Multidimensional neuroanatomical subtyping of autism spectrum disorder. *Cereb Cortex.* 28:3578–3588.
- Insel TR. 2014. The NIMH Research Domain Criteria (RDoC) Project: precision medicine for psychiatry. *Am J Psychiatry.* 171:395–397.
- Jbabdi S, Sotiropoulos SN, Haber SN, Van Essen DC, Behrens TE. 2015. Measuring macroscopic brain connections in vivo. *Nat Neurosci.* 18:1546–1555.
- Jenkinson M, Bannister P, Brady M, Smith S. 2002. Improved optimization for the robust and accurate linear registration and motion correction of brain images. *Neuroimage.* 17: 825–841.
- Jones DK, Knosche TR, Turner R. 2013. White matter integrity, fiber count, and other fallacies: the do's and don'ts of diffusion MRI. *Neuroimage.* 73:239–254.
- Joshi G, Arnold Anteraper S, Patil KR, Semwal M, Goldin RL, Furtak SL, Chai XJ, Saygin ZM, Gabrieli JDE, Biederman J, et al. 2017. Integration and segregation of default mode network resting-state functional connectivity in transition-age males with high-functioning autism spectrum disorder: a proof-of-concept study. *Brain Connect.* 7:558–573.
- Kana RK, Keller TA, Cherkassky VL, Minshew NJ, Just MA. 2009. Atypical frontal-posterior synchronization of Theory of Mind regions in autism during mental state attribution. *Soc Neurosci.* 4:135–152.
- Kennedy DP, Courchesne E. 2008. Functional abnormalities of the default network during self- and other-reflection in autism. *Soc Cogn Affect Neurosci.* 3:177–190.
- Keown CL, Shih P, Nair A, Peterson N, Mulvey ME, Muller RA. 2013. Local functional overconnectivity in posterior brain regions is associated with symptom severity in autism spectrum disorders. *Cell Rep.* 5:567–572.
- Khundrakpam BS, Lewis JD, Kostopoulos P, Carbonell F, Evans AC. 2017. Cortical thickness abnormalities in autism spectrum disorders through late childhood, adolescence, and adulthood: a large-scale MRI study. *Cereb Cortex.* 27: 1721–1731.
- Koldewyn K, Yendiki A, Weigelt S, Gweon H, Julian J, Richardson H, Malloy C, Saxe R, Fischl B, Kanwisher N. 2014. Differences in the right inferior longitudinal fasciculus but no general disruption of white matter tracts in children with autism spectrum disorder. *Proceedings of the National Academy of Sciences.* 111:1981–1986.
- Larivière S, Vos de Wael R, Paquola C, Hong SJ, Misić B, Bernasconi N, Bernasconi A, Bonilha L, Bernhardt B. 2018. Microstructure-informed connectomics: enriching large-scale descriptions of healthy and diseased brains. *Brain Connect.*
- Lerch J. 2005. In-vivo analysis of cortical thickness using magnetic resonance images [PhD]. [Montreal]: McGill University. (p. 214).
- Liu M, Bernhardt BC, Hong SJ, Caldaïrou B, Bernasconi A, Bernasconi N. 2016. The superficial white matter in temporal lobe epilepsy: a key link between structural and functional network disruptions. *Brain.* 139:2431–2440.
- Lombardo MV, Chakrabarti B, Bullmore ET, Baron-Cohen S. 2011. Specialization of right temporo-parietal junction for mentalizing and its relation to social impairments in autism. *Neuroimage.* 56:1832–1838.
- Lord C, Risi S, Lambrecht L, Cook EH Jr., Leventhal BL, DiLavore PC, Pickles A, Rutter M. 2000. The autism diagnostic observation schedule-generic: a standard measure of social and communication deficits associated with the spectrum of autism. *J Autism Dev Disord.* 30:205–223.
- Lord C, Rutter M, Le Couteur A. 1994. Autism Diagnostic Interview-Revised: a revised version of a diagnostic interview for caregivers of individuals with possible pervasive developmental disorders. *J Autism Dev Disord.* 24:659–685.
- Makowski C, Lewis JD, Tardif CL, Joobar R, Malla AK, Shah J, Chakravarty MM, Evans AC, Lepage M. 2018. S231. Intracortical and superficial white matter microstructural changes after a first episode of psychosis. *Biol Psychiatry.* 83:S438.
- Mar RA. 2011. The neural bases of social cognition and story comprehension. *Annu Rev Psychol.* 62:103–134.
- Mitchell JP, Macrae CN, Banaji MR. 2006. Dissociable medial prefrontal contributions to judgments of similar and dissimilar others. *Neuron.* 50:655–663.
- Nazeri A, Chakravarty MM, Rajji TK, Felsky D, Rotenberg DJ, Mason M, Xu LN, Lobaugh NJ, Mulsant BH, Voineskos AN. 2015. Superficial white matter as a novel substrate of age-related cognitive decline. *Neurobiol Aging.* 36:2094–2106.
- Oishi K, Huang H, Yoshioka T, Ying SH, Zee DS, Zilles K, Amunts K, Woods R, Toga AW, Pike GB, et al. 2011. Superficially located white matter structures commonly seen in the human and the macaque brain with diffusion tensor imaging. *Brain Connectivity.* 1:37–47.
- Oishi K, Zilles K, Amunts K, Faria A, Jiang H, Li X, Akhter K, Hua K, Woods R, Toga AW, et al. 2008. Human brain white matter atlas: identification and assignment of common anatomical structures in superficial white matter. *Neuroimage.* 43: 447–457.
- Parazzini C, Baldoli C, Scotti G, Triulzi F. 2002. Terminal zones of myelination: MR evaluation of children aged 20–40 months. *AJNR Am J Neuroradiol.* 23:1669–1673.
- Parent A, Carpenter MB. 1996. *Carpenter's human neuroanatomy.* Baltimore, MD: Williams & Wilkins.
- Phillips OR, Clark KA, Luders E, Azhir R, Joshi SH, Woods RP, Mazziotta JC, Toga AW, Narr KL. 2013. Superficial white

- matter: effects of age, sex, and hemisphere. *Brain Connect.* 3:146–159.
- Phillips OR, Joshi SH, Piras F, Orfei MD, Iorio M, Narr KL, Shattuck DW, Caltagirone C, Spalletta G, Di Paola M. 2016. The superficial white matter in Alzheimer's disease. *Hum Brain Mapp.* 37:1321–1334.
- Phillips OR, Joshi SH, Squitieri F, Sanchez-Castaneda C, Narr K, Shattuck DW, Caltagirone C, Sabatini U, Di Paola M. 2016. Major Superficial White Matter Abnormalities in Huntington's Disease. *Front Neurosci.* 10:197.
- Power JD, Barnes KA, Snyder AZ, Schlaggar BL, Petersen SE. 2012. Spurious but systematic correlations in functional connectivity MRI networks arise from subject motion. *Neuroimage.* 59:2142–2154.
- Ritchie SJ, Cox SR, Shen X, Lombardo MV, Reus LM, Alloza C, Harris MA, Alderson HL, Hunter S, Neilson E, et al. 2018. Sex differences in the adult human brain: evidence from 5216 UK Biobank participants. *Cereb Cortex.* 28:2959–2975.
- Saxe R, Kanwisher N. 2003. People thinking about thinking people. The role of the temporo-parietal junction in "theory of mind". *Neuroimage.* 19:1835–1842.
- Schaer M, Ottet MC, Scariati E, Dukes D, Franchini M, Eliez S, Glaser B. 2013. Decreased frontal gyrification correlates with altered connectivity in children with autism. *Front Human Neurosci.* 7:750.
- Schurz M, Radua J, Aichhorn M, Richlan F, Perner J. 2014. Fractionating theory of mind: a meta-analysis of functional brain imaging studies. *Neurosci Biobehav Rev.* 42:9–34.
- Schüz A, Braitenberg V. 2002. The human cortical white matter: quantitative aspects of cortico-cortical long-range connectivity, cortical areas: unity and diversity. London; New York: Taylor & Francis.
- Stoner R, Chow ML, Boyle MP, Sunkin SM, Mouton PR, Roy S, Wynshaw-Boris A, Colamarino SA, Lein ES, Courchesne E. 2014. Patches of disorganization in the neocortex of children with autism. *N Engl J Med.* 370:1209–1219.
- Taylor PA, Alhamud A, van der Kouwe A, Saleh MG, Laughton B, Meintjes E. 2016. Assessing the performance of different DTI motion correction strategies in the presence of EPI distortion correction. *Hum Brain Mapp.* 37:4405–4424.
- Toro R, Burnod Y. 2005. A Morphogenetic Model for the Development of Cortical Convolutions. *Cereb Cortex.* 15:1900–1913.
- Travers BG, Adluru N, Ennis C, Tromp do PM, Destiche D, Doran S, Bigler ED, Lange N, Lainhart JE, Alexander AL. 2012. Diffusion tensor imaging in autism spectrum disorder: a review. *Autism Res.* 5:289–313.
- Uddin LQ, Supekar K, Amin H, Rykhlevskaia E, Nguyen DA, Greicius MD, Menon V. 2010. Dissociable connectivity within human angular gyrus and intraparietal sulcus: evidence from functional and structural connectivity. *Cereb Cortex.* 20:2636–2646.
- Uddin LQ, Supekar K, Menon V. 2013. Reconceptualizing functional brain connectivity in autism from a developmental perspective. *Front Hum Neurosci.* 7:458.
- Valk SL, Bernhardt BC, Bockler A, Kanske P, Singer T. 2016. Substrates of metacognition on perception and metacognition on higher-order cognition relate to different subsystems of the mentalizing network. *Hum Brain Mapp.* 37:3388–3399.
- Valk SL, Bernhardt BC, Bockler A, Trautwein FM, Kanske P, Singer T. 2017. Socio-Cognitive Phenotypes Differentially Modulate Large-Scale Structural Covariance Networks. *Cereb Cortex.* 27:1358–1368.
- Valk SL, Bernhardt BC, Trautwein FM, Bockler A, Kanske P, Guizard N, Collins DL, Singer T. 2017. Structural plasticity of the social brain: Differential change after socio-affective and cognitive mental training. *Sci Adv.* 3:e1700489.
- Valk SL, Di Martino A, Milham MP, Bernhardt BC. 2015. Multicenter mapping of structural network alterations in autism. *Human Brain Mapp.* 36:2364–2373.
- Van Overwalle F. 2009. Social cognition and the brain: a meta-analysis. *Hum Brain Mapp.* 30:829–858.
- van Rooij D, Anagnostou E, Arango C, Auzias G, Behrmann M, Busatto GF, Calderoni S, Daly E, Deruelle C, Di Martino A, et al. 2017. Cortical and Subcortical brain morphometry differences between patients with autism spectrum disorder and healthy individuals across the lifespan: results from the ENIGMA ASD working group. *Am J Psychiatry.* appiajp201717010100.
- van Rooij D, Anagnostou E, Arango C, Auzias G, Behrmann M, Busatto GF, Calderoni S, Daly E, Deruelle C, Di Martino A, et al. 2018. Cortical and subcortical brain morphometry differences between patients with autism spectrum disorder and healthy individuals across the lifespan: results from the ENIGMA ASD working group. *Am J Psychiat.* 175:359–369.
- Vergani F, Mahmood S, Morris CM, Mitchell P, Forkel SJ. 2014. Intralobar fibres of the occipital lobe: a post mortem dissection study. *Cortex.* 56:145–156.
- White T, Hilgetag CC. 2011. Gyrification and neural connectivity in schizophrenia. *Dev Psychopathol.* 23:339–352.
- Winkler AM, Sabuncu MR, Yeo BT, Fischl B, Greve DN, Kochunov P, Nichols TE, Blangero J, Glahn DC. 2012. Measuring and comparing brain cortical surface area and other areal quantities. *Neuroimage.* 61:1428–1443.
- Worsley K, Andermann M, Koulis T, MacDonald D, Evans A. 1999. Detecting changes in nonisotropic images. *Hum Brain Mapp.* 8:98–101.
- Worsley K, Taylor JE, Carbonell F, Chung MK, Duerden E, Bernhardt BC, Lyttelton OC, Boucher M, Evans AC. 2009. SurfStat: A Matlab toolbox for the statistical analysis of univariate and multivariate surface and volumetric data using linear mixed effects models and random field theory. *Neuroimage.* 47:S102.
- Wu M, Lu LH, Lowes A, Yang S, Passarotti AM, Zhou XJ, Pavuluri MN. 2014. Development of superficial white matter and its structural interplay with cortical gray matter in children and adolescents. *Hum Brain Mapp.* 35:2806–2816.
- Yahata N, Morimoto J, Hashimoto R, Lisi G, Shibata K, Kawakubo Y, Kuwabara H, Kuroda M, Yamada T, Megumi F, et al. 2016. A small number of abnormal brain connections predicts adult autism spectrum disorder. *Nat Commun.* 7:11254.
- Zhuo C, Ma X, Qu H, Wang L, Jia F, Wang C. 2016. Schizophrenia patients demonstrate both inter-voxel level and intra-voxel level white matter alterations. *PLoS One.* 11:e0162656.
- Zikopoulos B, Barbas H. 2010. Changes in prefrontal axons may disrupt the network in autism. *J Neurosci Nurs.* 30:14595–14609.
- Zikopoulos B, Barbas H. 2013. Altered neural connectivity in excitatory and inhibitory cortical circuits in autism. *Front Hum Neurosci.* 7:609.